Journal of Computer Science & Computational Mathematics, Volume 7, Issue 3, September 2017
DOI: 10.20967/jcscm.2017.03.003

Surface Tension Instability in a Horizontal Nanofluid Layer

A. A. Abdullah

Department of Mathematical Sciences, Faculty of Applied Science, Umm Al-Qura University,
7797 Alawali, 24372 2976, Makkah, Saudi Arabia
Corresponding author email: aamohammad@uqu.edu.sa

Abstract: What is investigated below is a linear stability analysis for the onset of Marangoni convection in a horizontal layer of a nanofluid heated. The effects of both Brownian motion and thermophoresis are joined by the model used for the nanofluid. While the top boundary is assumed to be a non-deformable free surface, the layer lower boundary is assumed to be a rigid surface. The resulting eigenvalue problem is solved numerically by expanding eigenfunctions as Chebyshev series, and critical Marangoni numbers are obtained for all modes of instability. The effects of Lewis number, Nusselt number, modified diffusivity ratio and modified particle density increment on the stability of the system are also investigated.

Keywords: Marangoni convection, nanofluid, linear stability, stationary convection.

1. Introduction

A new dimension in the study of thermal instability recently was opened as a new class of fluid called as "nanofluid". . It is a base fluid containing particles with size less than 100 nm. These ultrafine particles are uniformly and stably distributed. The common heat transfer fluids used as base fluids include water, kerosene, ester, ethylene glycol, hydrocarbons etc., while the nanoparticles used include metallic or metallic oxide particles (Cu, CuO, Al2O3), carbon nanotubes etc.

Suspending solid particles can increase the heat transfer properties of fluids in them. Many researchers (Masuda et al. [1]; Choi [2]; Eastman et al. [3]; Das et al. [4]; Buongiorno [5]; Jain et al. [6]) have found that adding nanoparticles to ordinary fluid will increase the thermal conductivity of the nanofluid.

The conservation equation of a non-homogeneous equilibrium model of a nanofluid was derived by Buongiorno [5] in conducting an extensive study of nanofluids. The effects of Brownian diffusion and thermophoresis were incorporated by this model. According to this model, many authors have conducted studies (e.g. Tzou [7, 8]; Nield and Kuznetsov [9, 10]; Kuznetsov and Nield [11,12]). A wide area on heat transfer in nanofluids is covered in a book by Das et al. [13] and a review article by Das and Choi [14].

There is a flow of nanofluid of great interest in several areas of modern science, engineering and technology, the chemical and nuclear industries and bio-mechanics. Naturally, nanofluids are occurring rather they are manufactured in laboratories. The option of base fluid and particle combination are dependent on the application of nanofluid that are used in industries such as coolants, lubricants, nano-drug delivery, heat exchangers and micro-channel heat sinks among other applications (Buongiorno and Hu [15]; Tsai and Chein [16]; Kleinstreuer et al. [17]).

Several authors have studied the convective instability of nanofluids. The convective instability driven by buoyancy and heat transfer characteristics of nanofluids were studied by Kim et al. [18] analytically. Considering the thermal instability of nanofluids (Rayeligh-Benard convection), based on Tzou [7, 8] nanofluids are less stable than regular fluids. Lately Nield and Kuznetsov [9, 10] and Kuznetsov and Nield [11, 12] investigated the onset of convection in a horizontal layer of a porous medium saturated by a nanofluid by a model for the nanofluid that integrates the effects of Brownian motion and thermophoresis. What Yadav et al. [19, 20] included considering the linear stability of Rayleigh-Benard convection in nanofluids without and with rotation, and they gained a sufficient condition for the presence of overstability. The convection onset in a viscoelastic nanofluid-saturated porous medium was investigated by Sheu [21] who displayed the possibility of oscillatory instability for both bottom and top heavy nanoparticle distributions. The onset of double-diffusive convection in a nanofluid layer was studied by Nield and Kuznetsov [22].

Yadav et al. [23] studied the internal heating effect on the onset of Darcy-Brinkman convection in a porous layer saturated by nanofluid. They showed the destabilizing effect caused by internal heat source on the system. The rotation effect on a horizontal layer of nanofluid saturated by a porous medium was noticed by Ramesh and Rana [24]. Additionally, Gupta et al. [25], Yadav et al. [26] and Mahajan and Arora [27] discussed on the effect of magnetic field on the thermal instability of nanofluids.

Based on these authors, the presence of a magnetic field performs to stabilize the related system. Yadav et al. [28], Agarwal and Bhadauria [29] and others have discussed on the rotating nanofluids.

Marangoni convection is induced by the dependence of surface tension on temperature. The initial work on Marangoni instability in a fluid layer heated from below was done by Pearson [30] who claimed that, rather than being a buoyancy driven flow, Benard cells are induced by the gradients of surface tension resulting from variations in temperature across the free surface. Based on Nield [31] for layers that are most 0.1 cm deep the buoyancy effect for most liquids can safely be neglected. Many studies for deformable and non-deformable surfaces (e.g. Takashima [32, 33]; Benguria and Depassier [34]; Wilson [35];

Shivakumara et al. [36]; Hashim and Arifin [37]; Shivakumara et al. [38]) have extended and polished the findings of Pearson and Nield.

A literature review showed that there is no conducted research on the effect of Marangoni convection in nanofluids. Therefore the present study objective is to investigating the thermal instability of Marangoni convection in a horizontal layer of a nanofluid.

2. Problem formulation

Consider an infinite horizontal layer of an incompressible nanofluid which is heated from below and is confined between the planes $x_3 = 0$ and $x_3 = d$. The nanofluid temperature, T, and the volumetric fraction of nanoparticles, φ, at the lower boundary and upper boundary are (T_0, φ_0) and (T_1, φ_1) respectively, where T_0, T_1, φ_0 and φ_1 are each assumed to be constant. Specifically, φ_0 will be treated as the reference volume fraction for nanoparticles. The bottom surface is assumed to be rigid and the top surface is assumed to be a non-deformable free surface on which the fluid motion is determined totally by the thermocapillary effect of the surface tension of the nanofluid, say $\gamma\ (T, \varphi)$. A coordinate frame is selected in which the x_3 axis is aligned vertically upwards.

The thermo-physical properties of nanofluids (density, viscosity, thermal conductivity and specific heat) are assumed to be constant in the analytical formulation, although the values assigned to these constants will depend on the operational temperature regime of the nanofluid and the volume fraction of nanoparticles. Buongiorno [5] treats the nanofluid as a two-component mixture (base fluid plus nanoparticles).

Based on the study of Buongiorno [5], Tzou [7, 8] and Nield and Kuznetsov [9] the leading equations for a nanofluid in the chemical reactions absence and in the thermophoresisis presence are

$$\nabla.\boldsymbol{V}=0 \tag{1}$$

$$\rho\left[\frac{\partial \boldsymbol{V}}{\partial t}+(\boldsymbol{V}.\nabla)\boldsymbol{V}\right]=-\nabla P+\mu\nabla^2\boldsymbol{V}, \tag{2}$$

$$\frac{\partial\varphi}{\partial t}+(\boldsymbol{V}.\nabla)\varphi=-\frac{1}{\rho_p}\nabla.J \tag{3}$$

$$\rho C_p\left[\frac{\partial T}{\partial t}+(V.\nabla)T\right]=-\nabla.q+h_p(T)\,\nabla.J \tag{4}$$

where $\boldsymbol{V}$ is the nanofluid velocity, P is the hydrostatic pressure, μ is the dynamic viscosity of the nanofluid, C_P is the nanofluid specific heat at constant pressure, $h_p(T)$ is the specific enthalpy of the nanoparticle material at temperature T. and $\rho=\varphi\rho_p+(1-\varphi)\rho_f$ is the density of the nanofluid expressed in terms of ρ_p (assumed constant), the density of the nanoparticles, and ρ_f (assumed constant), the density of the base fluid. This analysis ignores any buoyancy effect in the bulk of the nanofluid because the layer under consideration is very thin with depth d ≤ 0.001 m.

The vector $\boldsymbol{J}$ denotes the diffusion mass flux for the nanoparticles and is the sum of two diffusion terms (Brownian diffusion and thermophoresis), namely

$$j_p=j_B+j_T=-\rho_p(D_B\nabla\varphi+D_T\frac{\nabla T}{T}), \tag{5}$$

in which D_B and D_T represent respectively the Brownian diffusion coefficient of the nanoparticles and the thermophoretic diffusion coefficient with respective constitutive specifications

$$D_B=\frac{K_B T}{3\pi\mu_f d_p},\quad D_T=\frac{\mu_f}{\rho_f}\left(\frac{0.26\kappa_f}{2\kappa_f+\kappa_p}\right)\varphi, \tag{6}$$

where K_B is Boltzman's constant, μ_f is the viscosity of the fluid, d_p is the nanoparticle diameter, and κ_f and κ_p are respectively the thermal conductivities of the fluid and nanoparticles. Also $\boldsymbol{q}$ is the heat flux with constitutive equation

$$\boldsymbol{q}=-\kappa\nabla T+h_p\boldsymbol{J}\ , \tag{7}$$

where κ is the nanofluid thermal conductivity. When expression (5) for $\boldsymbol{J}$ and expression (7) for $\boldsymbol{q}$ are substituted into equations (3) and (4) the result is that

$$\frac{\partial\varphi}{\partial t}+(V.\nabla)\varphi=D_B\nabla^2\varphi+\frac{D_T}{T}\nabla^2 T \tag{8}$$

$$\rho C_{\boldsymbol{p}}\left[\frac{\partial T}{\partial t}+(\boldsymbol{V}.\nabla)T\right]=\kappa\nabla^2 T+\rho_{\boldsymbol{p}}\boldsymbol{c}_{\boldsymbol{p}}\left(D_B\nabla\varphi.\nabla T+\frac{D_T}{T}\nabla T.\nabla T\right), \tag{9}$$

where c_p (assumed constant) is the specific heat of the material constituting the nanoparticles. The replacement of the gradient of h_p with respect to temperature by c_p implicitly implies that h_p performs as a temperature non-constant function. Therefore, h_p is well approximated by the formula

$$h_p(T)\approx\varphi h_p(T_0)+c_p(T-T_0),\qquad c_p=\frac{dh_p(T_0)}{dT}. \tag{10}$$

2.1 Specification of boundary conditions

At the free surface $x_3 = d$ the heat flux obeys Newton's Law of Cooling, namely

$$q_3=h(T-T_1)\ \rightarrow\ \kappa\frac{\partial T}{\partial x_3}-h_p(T)\,J_3+h(T-T_1)=0, \tag{11}$$

where h is the heat transfer coefficient between the free surface and the atmosphere which is here assumed to be at temperature T_1. When $\boldsymbol{J}$ is replaced by its constitutive specification given in equation (5), the surface heat loss condition (11) becomes

$$(\kappa+\rho_p h_p(T)\frac{DT}{T})\frac{\partial T}{\partial x_3}+\rho_p h_p(T)D_B\frac{\partial\varphi}{\partial x_3}+h(T-T_1)=0. \tag{12}$$

The final boundary conditions for the non-deformable (upper) free surface at $x_3 = d$ comprise a kinematic condition, a balance of tangential stress with surface tension, a heat loss condition to the region $x_3 > d$ at temperature T_1 and a volume fraction condition with the respective mathematical forms

$$V_3=0, \tag{13}$$

$$\mu\frac{\partial^2 V_3}{\partial {x_3}^2}=\gamma\,(\frac{\partial^2 T}{\partial {x_1}^2}+\frac{\partial^2 T}{\partial {x_2}^2})\,, \tag{14}$$

$$(\kappa+\rho_p\, h_p(T)\frac{D_T}{T})\frac{\partial T}{\partial x_3}++\rho_p\, h_p(T)\, D_B\frac{\partial \varphi}{\partial x_3}+h(T-T_1)=0\,, \tag{15}$$

$$\varphi=\varphi_1, \tag{16}$$

in which V_3 is the third component of velocity. The boundary conditions for the (lower) rigid surface $x_3 = 0$ are

$$V_3=0,\qquad \frac{\partial V_3}{\partial x_3}=0,\qquad T=T_0,\qquad \varphi=\varphi_0\,. \tag{17}$$

The Dirichlet boundary conditions imposed on volume fraction of nanoparticles is somewhat arbitrary. However Nield and Kuznetsov [9] explained that zero particle flux on the boundaries is more realistic physically, but then one is faced with the problem that no steady-state solution for the basic conduction equations is then possible, so that in order to make analytical progress it is necessary to freeze the basic profile for the volume fraction of nanoparticles and so our choice of boundary conditions is seen to be quite realistic.

2.2 Nondimensionlisation process

Let $\alpha=\kappa/\rho C_p$. In keeping with standard mathematical procedure, the model equations are now reformulated in terms of the non-dimensional variables

$$\begin{gathered} x^*=x/d,\qquad V^*=V\,d/\alpha,\qquad t^*=t\,\alpha/d^2,\\ P^*=P\,d^2/\mu\alpha,\qquad \varphi^*=\frac{\varphi-\varphi_0}{|\varphi_1-\varphi_0|},\qquad \varphi^*=\frac{T-T_0}{|T_1-T_0|}. \end{gathered} \tag{18}$$

The non-dimensional forms of equations (1), (2), (8) and (9) after dropping the asterisks become

$$\nabla.V=0\,, \tag{19}$$

$$\frac{1}{P_r}\left[\frac{\partial V}{\partial t}+(V.\nabla)V\right]=-\nabla P+\nabla^2 V, \tag{20}$$

$$Le\left(\frac{\partial \varphi}{\partial t}+(V.\nabla)\varphi\right)=\nabla.\left((1+\xi T)\nabla\varphi+N_A\frac{1+\lambda\varphi}{1+\xi T}\nabla T\right), \tag{21}$$

$$\frac{\partial T}{\partial t}+(V.\nabla)T=\nabla^2 T+\eta\big((1+\xi T)\nabla T.\nabla\varphi\big)+N_A\frac{1+\lambda\varphi}{1+\xi T}(\nabla T.\nabla T)), \tag{22}$$

where the Lewis number Le, the modified diffusivity ratio N_A, the Prandtl number Pr and the modified particle density increment N_B are defined by

$$\begin{gathered} Le=\frac{3\pi\alpha\mu_f\, d_p}{k\,T_0},\qquad N_A=\frac{D_{T_0}\,|T_1-T_0|}{D_{B_0}\,T_0\,|\varphi_1-\varphi_0|},\\ \mathrm{Pr}=\frac{\mu C_p}{\kappa},\qquad N_B=\frac{\rho_p\,c_p}{\rho C_p}|\varphi_1-\varphi_0|. \end{gathered} \tag{23}$$

The parameters η,λ and ξ are defined by

$$\eta=\frac{N_B}{Le},\qquad \lambda=\frac{|\varphi_1-\varphi_0|}{\varphi_0},\qquad \xi=\frac{|T_1-T_0|}{T_0}. \tag{24}$$

The corresponding non-dimensional form of the boundary conditions on $x_3 = 1$ becomes

$$V_3=0, \tag{25}$$

$$\frac{\partial^2 V_3}{\partial {x_3}^2}=M(\frac{\partial^2 T}{\partial {x_1}^2}+\frac{\partial^2 T}{\partial {x_2}^2}) \tag{26}$$

$$\begin{gathered}\frac{\partial T}{\partial x_3}+\eta(T+\frac{1}{R_h})\left((1+\xi T)\frac{\partial \varphi}{\partial x_3}+N_A\frac{1+\lambda\varphi}{1+\xi T}\frac{\partial T}{\partial x_3}\right)\\ =Nu\,\big(T-sign(T_1-T_0)\big)=0\end{gathered} \tag{27}$$

$$\varphi=sign(\varphi_1-\varphi_0), \tag{28}$$

where the Marangoni number M, the Nusselt number Nu and the relative change in enthalpy of the nanoparticles, R_h, are defined by

$$M=\frac{\gamma\,|T_1-T_0|\,d}{\alpha\,\mu},\qquad Nu=\frac{h\,d}{\kappa},\qquad R_h=\frac{c_p\,|T_1-T_0|}{h_p} \tag{29}$$

It is worth mentioning that data on the behavior of surface tension with volume fraction is sparse and conflicting. Experimental studies for different nanofluids have reported that the presence of nanoparticles causes surface tension to be increased (Zhu et al., [39]; Tanvir and Qiao, [40]; Lu et al., [41]), to be unchanged (Kumar and Milanova, [42]; Chen et al., [43]) or to be decreased (Das et al., [44]; Vafaei et al., [45]). For this reason this article has ignored any dependence of surface tension on nanoparticle volume fraction in the boundary conditions.

The boundary conditions for the rigid surface $x_3 = 0$ are

$$V_3=0,\qquad \frac{\partial V_3}{\partial x_3}=0,\qquad T=0,\qquad \varphi=0 \tag{30}$$

However, in practice λ and ξ are very small, and in keeping with the literature, all analyses to follow will consider the limiting case in which $\lambda\to 0$ and $\xi\to 0$. In this case the non-dimensional equations (19- 22) become

$$\nabla.V=0 \tag{31}$$

$$\frac{1}{P_r}\left[\frac{\partial V}{\partial t}+(V.\nabla)V\right]=-\nabla P+\nabla^2 V, \tag{32}$$

$$Le\left(\frac{\partial \varphi}{\partial t}+(V.\nabla)\varphi\right)=\nabla^2\varphi+N_A\nabla^2 T\,, \tag{33}$$

$$\frac{\partial T}{\partial t}+(V.\nabla)T=\nabla^2 T+\eta(\nabla T.\nabla\varphi+N_A(\nabla T.\nabla T)), \tag{34}$$

with non-dimensional surface boundary conditions on $x_3 = 1$ given by the equations

$$V_3=0, \tag{35}$$

$$\frac{\partial^2 V_3}{\partial {x_3}^2}=M(\frac{\partial^2 T}{\partial {x_1}^2}+\frac{\partial^2 T}{\partial {x_2}^2}) \tag{36}$$

$$\frac{\partial T}{\partial x_3}+\eta(T+\frac{1}{R_h})\left(\frac{\partial \varphi}{\partial x_3}+N_A\frac{\partial T}{\partial x_3}\right)+Nu\big(T-sign(T_1-T_0)\big)=0 \tag{37}$$

$$\varphi=sign(\varphi_1-\varphi_0), \tag{38}$$

and the non-dimensional base boundary conditions

$$V_3=0,\qquad \frac{\partial V_3}{\partial x_3}=0,\qquad T=0,\qquad \varphi=0\quad \text{on } x_3 = 0. \tag{39}$$

3. Basic solution

The basic state of the nanofluid layer is one in which the fluid is at rest with temperature and volume fraction that are functions of depth alone, that is,

$$V=0, \qquad T=T(x_3), \qquad \varphi=\varphi(x_3)\ . \tag{40}$$

In this case the pressure P is a constant function and the functions T and φ satisfy equations

$$\frac{d^2}{dx_3^2}\left(\varphi+N_A T\right)=0, \tag{41}$$

$$\frac{d^2T}{dx_3^2}+\eta\frac{dT}{dx_3}\left(\frac{d\varphi}{dx_3}+N_A\frac{dT}{dx_3}\right)=0. \tag{42}$$

together with the upper (surface) boundary conditions (35-38) and the lower (base) boundary conditions (39). Equation (41) is integrated immediately to deduce that

$$\frac{d\varphi}{dx_3}+N_A\frac{dT}{dx_3}=A, \tag{43}$$

where A is an unknown constant. Result (43) simplifies equation (42) which is then integrated twice to deduce that

$$T=\frac{B}{\eta}(1-e^{-\eta A x_3}), \tag{44}$$

where B is another unknown constant and it is noted that the stated solution satisfies the boundary condition $T(0) = 0$. A further integration of equation (43) yields the formal solution

$$\varphi(x_3)=Ax_3-N_A T(x_3)=Ax_3-\frac{N_A B}{\eta}(1-e^{-\eta A x_3}), \tag{45}$$

where A and B are unknown constants to be determined from equations (37) and (38), namely

$$f(A,B)=AB+\frac{\eta A}{R_h}+Nu\left(\frac{B}{\eta}(1-e^{-\eta A})-sign(T_1-T_0)\right)=0, \tag{46}$$

$$g(A,B)=A-\frac{N_A B}{\eta}(1-e^{-\eta A})-sign(\varphi_1-\varphi_0)=0. \tag{47}$$

Perhaps the most straightforward strategy to solve equations (46) and (47) is first to express B in terms of A to get

$$B=\frac{\eta(A-sign(\varphi_1-\varphi_0))}{N_A(1-e^{-\eta A})}, \tag{48}$$

and thereafter substitute this expression for B in equation (46) to get that A is the solution of the equation $\psi(A) = 0$ where

$$\psi(A)=\frac{\eta A(A-sign(\varphi_1-\varphi_0))}{N_A(1-e^{-\eta A})}+\frac{\eta A N_A}{R_h}$$
$$+Nu\left(A-sign(\varphi_1-\varphi_0)-N_A\, sign(T_1-T_0)\right). \tag{49}$$

The cases to be considered are divided into the direction of heating, namely from above or from below, and independently, the boundary with the larger nanoparticle density, namely the top boundary or the bottom boundary. However, independently of the particular configuration of heating and distribution of nanoparticle density, it is clear that $\psi(A)$ is a continuous function satisfying the properties

$$\psi(1+N_A)>0, \qquad \psi(-1-N_A)<0, \tag{50}$$

thereby ensuring that equation (49) always has a solution in the interval $(-1 - N_A, 1 + N_A)$. The associated value of B is calculated from expression (48).

When the value of η is small, which Buongiorno [5] states it is typically the case for most nanofluids, then equation (49) is solved for the value of A by numerical methods, and the associated value of B is then calculated from expression (48). Its clear from the asymptotic expressions for $T(x_3)$ and $\varphi(x_3)$ in equations (44) and (45) that both functions are well approximated by parabolas connecting the origin to $(1, AB(1-\frac{A\eta}{2}))$ and $(1, 1)$ respectively.

4. Perturbation equations

The linear stability of the system defined by equations (31-34) with boundary conditions (35 - 38) and (39) is investigated by perturbing the base solution

$$V=0, \qquad T=T(x_3), \qquad P=P(x_3), \qquad \varphi=\varphi(x_3), \tag{51}$$

with the infinitesimal small perturbations εv, $\varepsilon p(x_3)$, $\varepsilon\theta$ and $\varepsilon\psi$ respectively. Thus

$$\nabla.v=0 \tag{52}$$

$$\frac{1}{P_r}\frac{\partial v}{\partial t}=-\nabla P+\nabla^2 v, \tag{53}$$

$$Le\left(\frac{\partial\varphi}{\partial t}+(V.\nabla)\varphi\right)=\nabla^2\varphi+N_A\nabla^2 T\ , \tag{54}$$

$$\frac{\partial\theta}{\partial t}+(v.\nabla)T=\nabla^2\theta+\eta(\nabla T.\nabla\varphi+N_A(\nabla T.\nabla T)), \tag{55}$$

with non-dimensional surface boundary conditions

$$v_3=0, \tag{56}$$

$$\frac{\partial^2 v_3}{\partial x_3{}^2}=M\left(\frac{\partial^2 T}{\partial x_1{}^2}+\frac{\partial^2 T}{\partial x_2{}^2}\right) \tag{57}$$

$$\frac{\partial T}{\partial x_3}+\eta(T+\frac{1}{R_h})\left(\frac{\partial\varphi}{\partial x_3}+N_A\frac{\partial T}{\partial x_3}\right)+Nu\left(T-sign(T_1-T_0)\right)=0 \tag{58}$$

$$\varphi=sign(\varphi_1-\varphi_0), \tag{59}$$

on $x_3 = 1$, and non-dimensional base boundary condition

$$v_3=0, \qquad \frac{\partial v_3}{\partial x_3}=0, \qquad T=0, \qquad \varphi=0 \quad \text{on } x_3 = 0. \tag{60}$$

4.1 Normal mode analysis

A normal mode analysis is used in which

$$(v_3,T,\varphi)=\left[w(x_3),\theta(x_3),\phi(x_3)\right]\exp(inx_1+imx_2+\sigma t) \tag{61}$$

where n, m are the wave numbers along the $\boldsymbol{e_1}$ and $\boldsymbol{e_2}$ directions respectively and σ is a growth rate. The hydrostatic pressure is eliminated from equation (53) by two applications of the curl operator. Thus the third component of equations (53-55) give

$$\sigma Lw=P_r L^2 w, \tag{62}$$

$$\sigma\phi=\frac{1}{Le}L\phi+\frac{1}{Le}N_A L\theta-w, \qquad (63)$$

$$\sigma\theta=L\theta+\frac{N_B}{Le}\left(1-2N_A\frac{N_u}{1+N_u}\right)D\theta$$

$$-\frac{N_B}{Le}\frac{N_u}{1+N_u}D\phi+\frac{N_u}{1+N_u}w. \qquad (64)$$

These equations are to be solved with the non-dimensional surface boundary conditions

$$w=0,\quad D^2w=-a^2M\theta,\quad D\theta+N_u\theta=0,\quad \phi=0,\quad \text{on } x_3=1 \qquad (65)$$

$$w=0,\qquad Dw=0,\qquad \theta=0,\qquad \psi=0,\quad \text{on } x_3=0 \qquad (66)$$

where

$$D=\frac{d}{dx_3},\qquad L=D^2-a^2,\qquad a=\sqrt{(n^2+m^2)}$$

4.2 Numerical procedure

The governing equations (62-64) together with the boundary conditions (65) and (66) are solved numerically when the nanofluid layer is heated from below and the nanoparticle density is greatest on the lower boundary. Numerical results are obtained by the Chebyshev spectral method. This procedure has high accuracy and allows simultaneous treating of stationary and overstable modes , which is useful when the critical eigenvalue flits between stationary and overstable modes in response to changing parameter values.

We _first map $x_3 \epsilon (0, 1)$ and $x_3 \epsilon (-1, 0)$ into $z \epsilon (-1, 1)$ by the transformations z = 2x$_3$ - 1 and z = 2x$_3$ + 1 respectively, then we suppose that

$$y_r(z)=\sum_{k=0}^{N-1}a_{kr}T_k(z),\quad 1\le r\le 8,\quad z\in(-1,1)$$

to be the Chebyshev expansion of the variables y_r which are defined by

$$y_1=w,\quad y_2=Dw,\quad y_3=D^2w,\quad y_4=D^3w,$$

$$y_5=\theta,\quad y_6=D\theta,\quad y_7=\varphi,\quad y_8=D\varphi,$$

where N is the number of Chebyshev polynomials used for the required accuracy. Equations (62 - 64) can be rewritten as an eigenvalue problem of the form $AY = \sigma BY$. This generalized matrix eigenvalue problem is solved using the QZ algorithm via the NAG routine F02BJF. In this case each eigenvector corresponds to the spectral coefficients of the physical mode associated with a given eigenvalue.

5. Results and discussion

The eigenvalues of this problem are expected to be complex valued. Given values for N_A, N_B, Le, Nu, Pr and R_h the task is to determine the critical value for the Marangoni Number M below which all eigenvalues have negative real parts. If the critical eigenvalue is real, then instability would occur by stationary convection. On the other hand if the critical eigenvalue is one of a complex conjugate pair of eigenvalues, then instability would occur by overstable convection.

The neutral stability curves in the (a, M_c) plane separate regions of unstable modes from those of stable modes. These curves are shown in Figs. 1-5 at which the critical Marangoni number, M_c, and the corresponding wave number, a, are displayed for different values of the physical parameters N_A, N_B, Le, Nu, Pr and R_h. From these figures it is clear that the linear stability criteria can be expressed in terms of the critical Marangoni number, M_c, below which the system is stable and above it the system is unstable.

Fig. 1 shows the neutral stability curves for different values of the diffusivity ratio, N_A when $Pr = 1$, $Le = 500$, $N_B = 2$, $R_h = -0.1$ and $Nu = 100$. The curves indicate that the critical Marangoni number, M_c, decreases as the modified diffusivity ratio increases. Thus the effect of increasing N_A is to destabilize the system. The neutral stability curves for different values of the particle increment parameter, N_B, are displayed in Fig. 2 when $Pr = 1$, $Le = 500$, $N_A = 5$, $R_h = -0.1$ and $Nu = 100$. Clearly the critical Marangoni number, M_c, decreases as the particle increment parameter, N_B, increases which indicates that increasing the particle density increment destabilizes the system since the heavier nanoparticles which move through the base fluids make stronger disturbances by comparison with lighter nanoparticles. i.e. Brownian motion promotes disturbances in nanofluid. Moreover the values of the critical Marangoni number for alumina/water nanofluid, $N_B = 0.2$, are higher by comparison with the values of critical Marangoni number for copper/water nanofluid, $N_B = 2$. Hence the alumina-water nanofluid are more stable than the copper-water nanofluid.

Fig. 3 shows the neutral stability curves for different values of the Nusslet number, Nu, when $Pr = 1$, $Le = 500$, $N_A = 5$, $R_h = -0.1$ and $N_B = 2$. The curves show that the critical Marangoni number, M_c, increases as the Nusslet number increases indicating that the Nusslet number has a stabilizing influence on the system. Fig. 4 shows the neutral stability curves for different values of Lewis number, Le, when $Pr = 1$ $Nu = 100$, $N_A = 5$, $R_h = -0.1$ and $N_B = 2$. The curves show that the critical Marangoni number, M_c, increases as the Lewis number increases again indicating that an increasing Lewis number has a stabilising influence.

The neutral stability curves for different values of the relative change in the enthalpy of the nanoparticles, R_h, are displayed in Fig. 5 when $Pr = 1$, $Le = 500$, $N_A = 5$, $Nu = 100$ and $N_B = 2$. For stability R_h must be negative (i.e. heat is released) and it is clear from Fig. 5 that the critical Marangoni number increases as R_h becomes more negative.

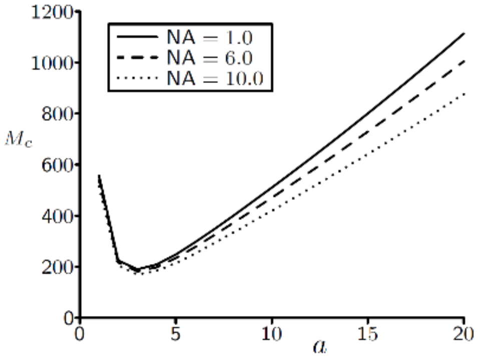

Figure 1. The neutral stability curves for different values of N_A

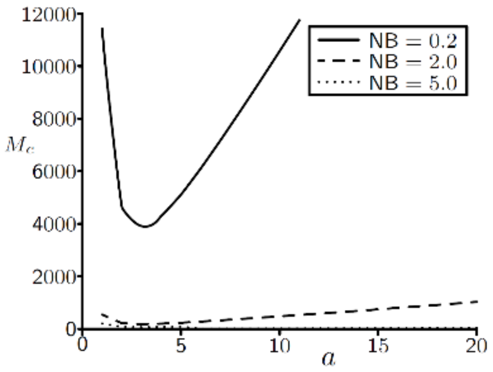

Figure 2. The neutral stability curves for different values of NB

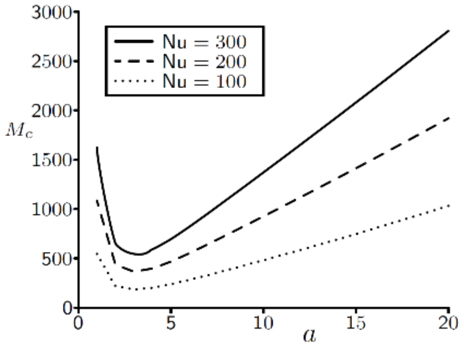

Figure 3. The neutral stability curves for different values of Nu

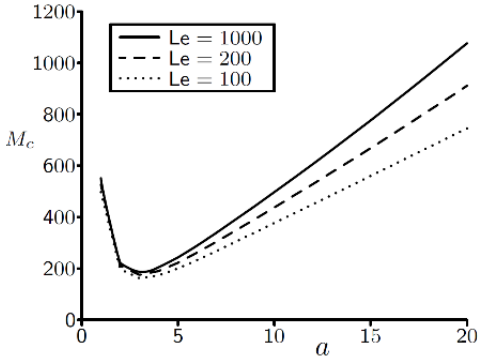

Figure 4. The neutral stability curves for different values of Le

The critical Marangoni numbers for different values of the nanofluid parameters are displayed in Figs. 6-10. These Figures show that the critical Marangoni number decreases as N_A, R_h or N_B increases and increases as *Le* or *Nu* increases. Fig. 10 shows that the critical Marangoni number increases sharply as R_h decreases, i.e. becomes more negative. When $R_h \leq -0.7$ the value of M_c settle at $M_c = 17655$.

Fig. 11 shows the critical Marangoni number for different values of the Nusslet number, *Nu*, for both nanofluids and regular fluids. Clearly the values of the critical Marangoni number for regular fluids are higher than the corresponding values for nanofluids indicating that regular fluids are more stable than nanofluids.

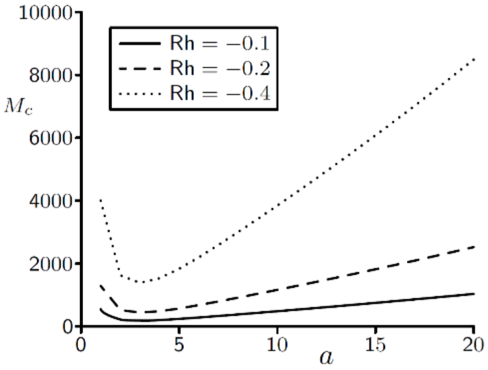

Figure 5. The neutral stability curves for different values of Rh

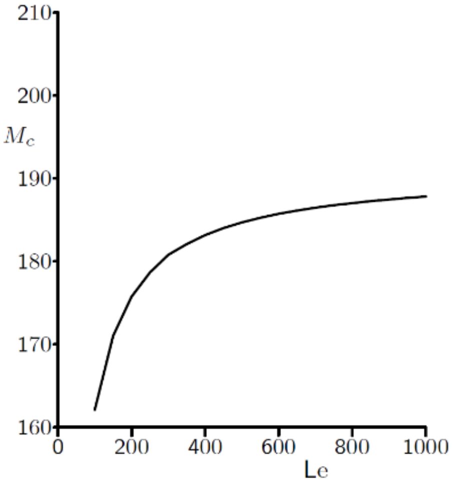

Figure 6. The relation between Mc and Le

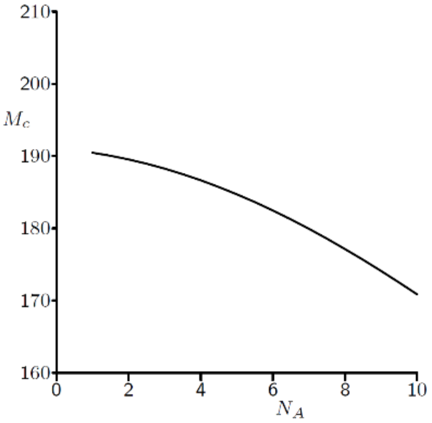

Figure 7. The relation between Mc and NA

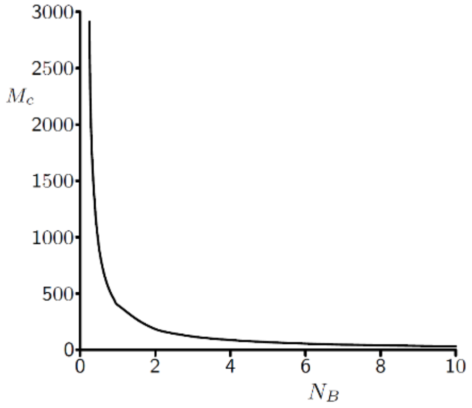

Figure 8. The relation between M_c and N_B

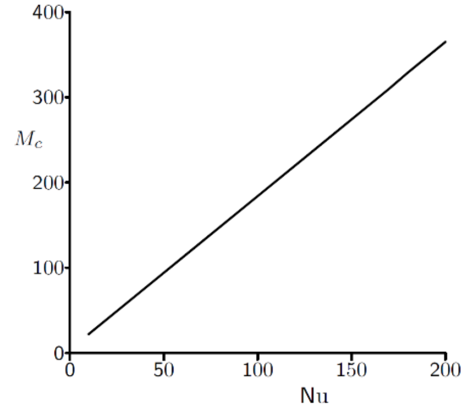

Figure 9. The relation between M_c and *Nu*

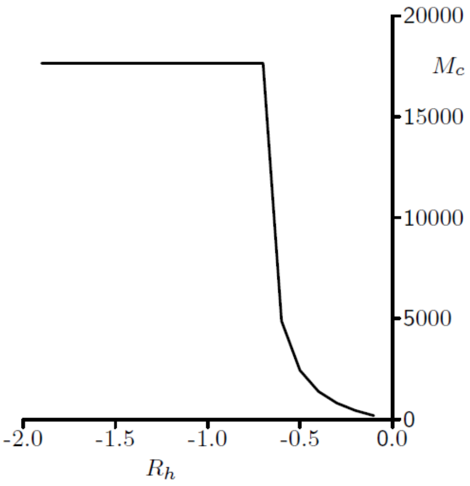

Figure 10. The relation between M_c and R_h

6. Results related to real nanofluids

The analysis of the preceding sections is now particularized to two nanofluids ethanol-alumina and dw-alumina. Table 1 gives the values used for the physical properties of the fluids (distilled water and ethanol) and alumina nanoparticles used in this work.

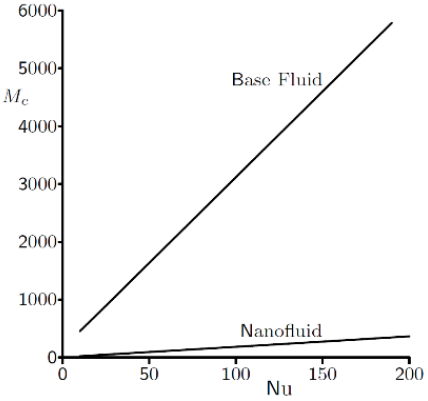

Figure 11. Relation between M_c and *Nu* for nanofluids and regular fluids

Table 1. Values for the various properties of distilled water, ethanol and alumina used in the calculations of this work.

Property	ρ	κ_f	C_p	μ	d_p
DW	1000	0.58	4184	0.00089	-
Ethanol	789	0.17	2460	0.00075	-
Alumina	3700	46	880	-	25

The non-dimensional parameters obtained in this work is calculated using the values of the physical properties of the two nanofluids and are listed in Table 2. Comparing these values with those proposed in the figures we found that the values proposed in the figures are acceptable for N_A, *Le* and *Pr* but for N_B they are large by two orders of magnitude and for N_u they are large by three orders of magnitude.

Table 2. Values of the non-dimensional parameters for dw-alumina and ethanol-alumina nanofluids.

Parameter	N_A	N_B	*Le*	N_u	*Pr*
DW-Alumina	0.961	0.0008	7018	0.017	6.42
Ethanol-Alumina	0.258	0.0017	3736	0.059	10.85

7. Conclusions

This study has examined the linear stability of Marangoni convection for a nanofluid layer heated from below and losing heat on its surface to a region at constant temperature. The model which is used for the nanofluid joins the effects of both Brownian motion and thermophoresis. The lower layer boundary of is assumed to be a rigid surface while the top boundary is assumed to be a non-deformable free surface. The resulting eigenvalue is handled using the method of expansion of Chebyshev polynomials.

The behaviour of various parameters like particle increment parameter, the diffusivity ratio, the Nusslet number, the relative change in the enthalpy of the nanoparticles and the Lewis number has been analysed numerically and results have been depicted graphically. The numerical results obtained showed that the presence of nanoparticles lowers the value of the critical Marangoni number.

Acknowledgment

The authors are thankful for this project financial support from King Abdulaziz City of Science and technology, Saudi Arabia through its National Science, Technology and Innovation Plan (Research project No. 12-MAT2296-10). The authors would like also to thank Professor Kenneth A. Lindsay from Glasgow University, Uk for his useful help and suggestions for improvement.

References

[1] H. Masuda, A. Ebata, K. Teramae, N. Hishinuma, “Alteration of thermal conductivity and viscosity of liquid by dispersing ultra-fine particles”, *Netsu Bussei* , vol 7, pp. 227-233, 1993.

[2] U. Choi, “Enhancing thermal conductivity of fluids with nanoparticles”, in : D. Siginer and H. Wang (Eds.), *Development and applications of non-Newtonian flows, ASME FED*, 231/MD-66 pp. 99-105, 1995.

[3] J. Eastman, S. Choi, S. Li, W. Yu, L. Thompson, “Anomalously increased effective thermal conductivities of ethylene glycol-based nanofluids containing copper nanoparticles”, *Applied Physics Letters*, vol. 78, no. 6, pp. 718-720, 2001.

[4] S. Das, N. Putra, W. Roetzel, “Pooling boiling characteristics of nano-fluids”, *International Journal of Heat and Mass Transfer*, vol. 46, no. 5, pp. 851-862, 2003.

[5] J. Buongiorno, “Convective transport in nanofluids”, *Journal of Heat Transfer. ASME*, vol. 128, no. 3, pp. 240-250, 2005.

[6] S. Jain, H. Patel, S. Das, “Brownian dynamic simulation for the prediction of effective thermal conductivity of nanofluid”, *Journal of Nanoparticle Research*, vol. 11, pp. 767-773, 2009.

[7] D. Y. Tzou, “Thermal instability of nanofluids in natural convection”, *International Journal of Heat and Mass Transfer*, vol. 51, no. 11-12, pp. 2967-2979, 2008.

[8] D. Y. Tzou, “Instability of nanofluids in natural convection”, *ASME Journal of Heat Transfer*, vol. 130, no. 7, 072401, pp. 1-8, 2008.

[9] D. A. Nield, A. V. Kuznetsov, “Thermal instability in a porous medium layer saturated by a nanofluid”, *International Journal of Heat and Mass Transfer*, vol. 52, no. 25-26, pp. 5796-5801, 2009.

[10] D. A. Nield, A. V. Kuznetsov, “The onset of convection in a horizontal nanofluid layer of finite depth”, *European Journal of Mechanics*, vol. 29, no. 3, pp. 217-223, 2010.

[11] A. V. Kuznetsov, D. A. Nield, “The onset of double diffusive nanofluid convection in a layer of a saturated porous medium”, *Transport. Porous Media*, vol. 85, no. 3, pp. 941-951, 2010.

[12] A. V. Kuznetsov, D. A. Nield, “Effect of local thermal non-equilibrium on the onset of convection in a porous medium layer saturated by a nanofluid”, *Transport. Porous Media*, vol. 83, no. 2, pp. 425-436, 2009.

[13] S. Das, S. Choi, W. Yu, T. Pradeep, “Nanofluids: Science and Technology”, *Wiley*, Hoboken, NY (2008).

[14] S. Das, S. Choi, “A review of heat transfer in nanofluids”, *Advances in Heat Transfer*, vol. 41, pp. 81-197, 2009.

[15] J. Buongiorno, L. Hu, “Nanofluid coolants for advanced nuclear power plants”, *Proceedings of ICAPP '05, Seoul, May 15-19*, Paper no. 5705, 2005.

[16] T. Tsai, R. Chein, “Performance analysis of nanofluid-cooled microchannel heat sinks”, *International Journal of Heat Fluid Flow*, vol. 28, no. 5, pp. 1013-1026, 2007.

[17] C. Kleinstreuer, J. Li, J. Koo, “Microfluidics of nano-drug delivery”, *International Journal of Heat and Mass Transfer*, vol. 51, no. 23-24, pp. 5590-5597, 2008.

[18] J. Kim, Y. Kang, C. Choi, “Analysis of convective instability and heat transfer characteristics of nanofluids”, *Phys. Fluids*, vol. 16, no. 7, pp. 2395-2401, 2004.

[19] D. Yadav, G. Agrawal, R. Bhargava, “Thermal instability of rotating nanofluid layer”, *International Journal of Engineering Science.*, vol. 49, no. 11, pp. 1171-1184, 2011.

[20] D. Yadav, G. Agrawal, R. Bhargava, “Rayleigh-Benard Convection in nanofluid”, *International Journal of Applied Mathematics and Mechanics*, vol. 7, no. 2, pp. 61-76, 2011.

[21] L. Sheu, “Thermal instability in a porous medium layer saturated with a viscoelastic nanofluid”, *Transport. Porous Media*, vol. 88, no. 3, pp. 461-477, 2011.

[22] D. A. Nield, A. V. Kuznetsov, “The onset of double-diffusive convection in a nanofluid layer”, *International Journal of Heat Fluid Flow*, vol. 32, no. 4, pp. 771-776, 2011.

[23] D. Yadav, R. Bhargava, G. Agrawal, “Boundary and internal heat source effects on the onset of Darcy-Brinkman convection in a porous layer saturated by nanofluid”, *International Journal of Thermal Sciences*, vol. 60, pp. 244-254, 2012.

[24] C. Ramesh, G. C. Rana, “On the onset of thermal convection in rotating nanofluid layer saturating a

Darcy-Brinkman porous medium", *International Journal of Heat and Mass Transfer*, vol. 55, no. 21-22, pp. 5417-5424, 2012.

[25] U. Gupta, J. Ahuja, R. Wanchoo, "Magneto convection in a nanofluid layer", *International Journal of Heat and Mass Transfer*, vol. 64, pp. 1163-1171, 2013.

[26] D. Yadav, R. Bhargava, G. Agrawal, "Thermal instability in a nanofluid layer with a vertical magnetic field", *Journal of Engineering Mathematics*, vol. 80, no. 1, pp. 147-164, 2013.

[27] A. Mahajan, M. Arora, "Convection in rotating magnetic nanofluids", *Applied Mathematics and Computation*, vol. 219, no. 11, pp. 6284-6296, 2013.

[28] D. Yadav, R. Bhargava, G. S. Agrawal, N. Yadav, J. Lee, M. C. Kim, "Thermal instability in a rotating porous layer saturated by a non-Newtonian nanofluid with thermal conductivity and viscosity variation", *Microfluid Nanofluid.*, vol.16, no. 1-2, pp. 425-440, 2013.

[29] S. Agarwal, B. Bhadauria, "Unsteady heat and mass transfer in a rotating nanofluid layer", *Continuum Mech. Thermodyn*., vol. 26, no. 4, pp. 437-445, 2013.

[30] J. Pearson, "On convection cells induced by surface tension", *Journal of Fluid Mechanics*, vol. 4, no. 5, pp. 489-500, 1958.

[31] D. A. Nield, "Surface tension and buoyancy effects in cellular convection", *Journal of Fluid Mechanics*, vol. 19, no. 3, pp. 341-352, 1964.

[32] M. Takashima, "Surface tension driven instability in a horizontal liquid layer with a deformable free surface I. Stationary convection", *Journal of the Physical Society of Japan*, vol. 50, no. 8, pp. 2745-2750, 1981.

[33] M. Takashima, "Surface tension driven instability in a horizontal liquid layer with a deformable free surface II. Overstability", *Journal of the Physical Society of Japan*, vol. 50, no. 8, pp. 2751-2756, 1981.

[34] R. Benguria, M. Depassier, "On the linear stability theory of Benard-Marangoni convection", *Phys. Fluids A.*, vol. 1, no. 7, pp. 1123-1127, 1989.

[35] S. Wilson, "The effect of a uniform magnetic field on the onset of steady Bénard-Marangoni convection in a layer of conducting fluid", *Journal of Engineering Mathematics*, vol. 27, no. 2, pp. 161-188, 1992.

[36] I. Shivakumara, M. Venkatachalappa, S. Summa, "Exact analysis of Marangoni convection with throughflow", *Acta Mech*, vol. 136, no. 1-2, pp. 109-117, 1998.

[37] I. Hashim, N. M. Arfin, "Oscillatory Marangoni convection in a conducting fluid layer with a deformable free surface in the presence of a vertical magnetic field", *Acta Mech.*, vol. 164, no. 3-4, pp. 199-215, 2003.

[38] I. Shivakumara, C. Nanjundappa, K. Chavaraddi, "Darcy-Benard-Marangoni convection in porous media", *International Journal of Heat and Mass Transfer*, vol. 52, no. 11-12, pp. 2815-2823, 2009.

[39] D. Zhu, S. Wu, M. Wang, "Thermal physics and critical heat flux characteristics of Al2O3-H2O nanofluids", *Heat Transfer Engineering*, vol. 31, no. 14, pp. 1213-1219, 2010.

[40] S. Tanvir, L. Qiao, "Surface tension of Nanofluid-type fuels containing suspended nanomaterials", *Nanoscale Research Letters*, vol. 7, pp. 226-235, 2012.

[41] G. Lu, Y. Duan, X. Wang, "Surface tension, viscosity, and rheology of water-based nanofluids: a microscopic interpretation on the molecular level", *Journal of Nanoparticle Research*, vol. 16, p. 2564, 2014.

[42] R. Kumar, D. Milanova, "Effect of surface tension on nanotube nanofluids", *Applied Physics Letters*, vol. 94, no. 7, p. 3107, 2014.

[43] R. Chen T. Phuoc, D. Martello, "Surface tension of evaporating nanofluid droplets", *International Journal of Heat and Mass Transfer*, vol. 54, no. 11-12, pp. 2459-2466, 2011.

[44] S. Das, N. Putra, W. Roetzel, "Pool boiling characteristics of nanofluids", *International Journal of Heat and Mass Transfer*, vol. 46, no. 5, pp. 851-862, 2003.

[45] S. Vafaei A. Purkayashtha, A. Jain, G. Ramanath, T. Borca-Tasciuc, "The effect of nanoparticles on the liquid-gas surface tension of Bi2Te3 nanofluids", *Nanotechnology*, vol. 20, no. 18, p. 185702, 2009.